Tailoring magnetic fields in inaccessible regions

Article (Accepted Version)

Tailoring magnetic fields in inaccessible regions

Rosa Mach-Batlle[1,2],* Mark G. Bason[3], Nuria Del-Valle[2], and Jordi Prat-Camps[4]
[1] *Departament de Fisica, Universitat Autonoma de Barcelona, Bellaterra 08193, Spain.*
[2] *Center for Biomolecular Nanotechnologies, Istituto Italiano di Tecnologia, Via Barsanti 14, 73010 Arnesano (LE), Italy.*
[3] *Department of Physics and Astronomy, University of Sussex, Falmer, Brighton BN1 9QH, United Kingdom.*
[4] *INTERACT Lab, School of Engineering and Informatics, University of Sussex, Brighton BN1 9QH, United Kingdom.*

Controlling magnetism, essential for a wide-range of technologies, is impaired by the impossibility of generating a maximum of magnetic field in free space. Here, we propose a strategy based on negative permeability to overcome this stringent limitation. We experimentally demonstrate that an active magnetic metamaterial can emulate the field of a straight current wire at a distance. Our strategy leads to an unprecedented focusing of magnetic fields in empty space and enables the remote cancellation of magnetic sources, opening an avenue for manipulating magnetic fields in inaccessible regions.

Magnetism is a physical phenomenon that is found at the basis of a wide range of technologies, from conventional motors and generators to sophisticated biomedical techniques and quantum technologies. In the last decade, the advent of metamaterials has enabled the manipulation of magnetic fields in unusual and extraordinary ways, leading to magnetic cloaks that can make objects magnetically undetectable [1, 2], magnetic hoses that can guide the magnetic field [3], and even magnetic wormholes that can connect two points through an undetectable path [4]. However, the degree of control one can exert over magnetic fields is restrained by some fundamental limitations. One of the most striking examples is the impossibility of generating local magnetic field maxima in free space, as stated by Earnshaw's theorem [5]. This strong limitation prevents the stable magnetostatic trapping of paramagnetic and ferromagnetic materials, limits the ability to concentrate magnetic fields, and makes it impossible to exactly create and cancel magnetic field sources, such as magnets or electric wires, at a distance. The creation of a magnetic source at a distance would open a new avenue for controlling and tailoring magnetic fields in inacessible regions, which would have deep impacts on several magnetic field-based, cutting-edge technologies. For example, it could improve the guidance of magnetic microrobots and functional nanoparticles for medical applications [6, 7], enhance techniques like transcranial magnetic stimulation [8] by providing strong and spatially-localized magnetic fields at target locations, open new avenues in atom trapping, or provide radical new ways of shielding undesired magnetic fields remotely.

Here, we demonstrate that the apparent impossibility of generating a source of static magnetic field remotely (such as a long wire, Fig. 1), which would not fulfill Earnshaw's theorem, can be circumvented by active negative-permeability media. Our approach is based on negative-permeability magnetic materials, a recently introduced class of material that exhibits appealing unconventional properties for manipulating magnetic fields [9]. While the counterpart of such media for controlling electromagnetic waves, media with a negative index of refraction or left-handed media, has been widely studied in the last decade due to their extraordinary ability focus electromagnetic waves beyond the diffraction limit [10], the potential of negative-permeability media for controlling static magnetic fields remains unexplored due to the impossibility of having passive materials with negative magnetic permeability in the static limit [11]. It has recently been demonstrated, however, that negative-permeability media can be effectively mimicked as active metamaterials consisting of precise arrangements of currents [12]. In this way, negative permeability media have been shown to be able to transform the magnetic signature of an object to make it appear as a different material (with different size or magnetic nature), providing a kind of magnetic illusion [9].

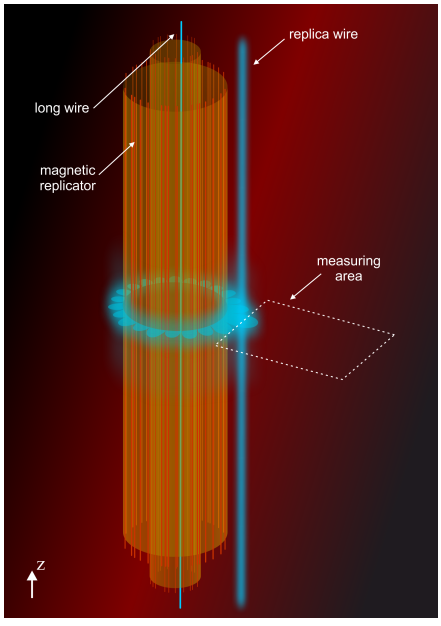

FIG. 1. A long wire is surrounded by a magnetic replicator generating a replica of the wire outside it.

Using transformation optics (see Supplemental Material), we demonstrate that a long cylindrical shell with relative magnetic permeability $\mu = -1$ acts analogously to a perfect lens for electromagnetic waves [13, 14] in the magnetostatic limit. When this negative-permeability shell surrounds a magnetic field source the field distribution outside the shell corresponds to the field created by another magnetic source, a *replica* source, which can appear at a distance from its external surface, i.e. in free space (see Fig. 1). A cylindrical shell with $\mu = -1$ can be mimicked by two surface current densities, $\mathbf{K}_{M_1}(\varphi)$ and $\mathbf{K}_{M_2}(\varphi)$, flowing on its internal and external surfaces, respectively [9, 12]. Our goal now is to demonstrate that these current densities can lead to the creation of a magnetic source at a distance. For the sake of generality, we focus on the creation of a wire; any other field source with translational symmetry along the device's axis can be regarded as the superposition of the field created by a combination of wires.

We solve the magnetostatic Maxwell's equations considering a long (along z) cylindrical shell with $\mu = -1$, internal radius R_1 and external radius R_2 which we coin a *magnetic replicator*. It surrounds a long (along z) straight wire of current I placed at $(x, y) = (d, 0)$. The solutions show that the magnetic field in the space beyond the replicator corresponds to the field created by a replica wire of current I placed at $(x, y) = (d', 0)$, where $d' = dR_2^2/R_1^2$. When the replica wire appears in empty space, $d' > R_2$, the field solution in the region $\rho \in (R_2, d')$, diverges [15, 16] (where ρ is the standard cylindrical radial coordinate). This annular region of divergent field solution makes it possible to have a divergence of the field at the position of the replica wire without having a local field maximum in empty space, thus ensuring that Earnshaw's theorem is obeyed.

From the field distribution, we obtain the current densities required to emulate a wire at a distance. Both $\mathbf{K}_{M_1}(\varphi)$ and $\mathbf{K}_{M_2}(\varphi)$ are found as an infinite series but, while $\mathbf{K}_{M_1}(\varphi)$ is always convergent, $\mathbf{K}_{M_2}(\varphi)$ only converges when the replica wire appears in the device volume ($d' \leq R_2$). The divergence of $\mathbf{K}_{M_2}(\varphi)$ in the cases in which the replica wire appears in empty space ($d' > R_2$) indicates that the exact creation of a magnetic source at a distance from the replicator would require infinite current at the external boundary of the device. However, numerical calculations demonstrate that one can still approximate well the field created by a wire at a distance by truncating the summation in $\mathbf{K}_{M_2}(\varphi)$ up to n_T terms. As shown in Fig. 2, the higher the number of terms n_T, the more the external field distribution resembles the field created by a wire [compare Figs. 2(a)-(c) with (d)]. By increasing n_T the spatial focusing of the B_y component is greatly improved [Fig. 2(e)] and both the B_x and the B_y components of the field rapidly converge to the distribution created by a wire [Fig. 2 (e) and (f)]. Therefore, the quantity n_T defines the accuracy of the replicator.

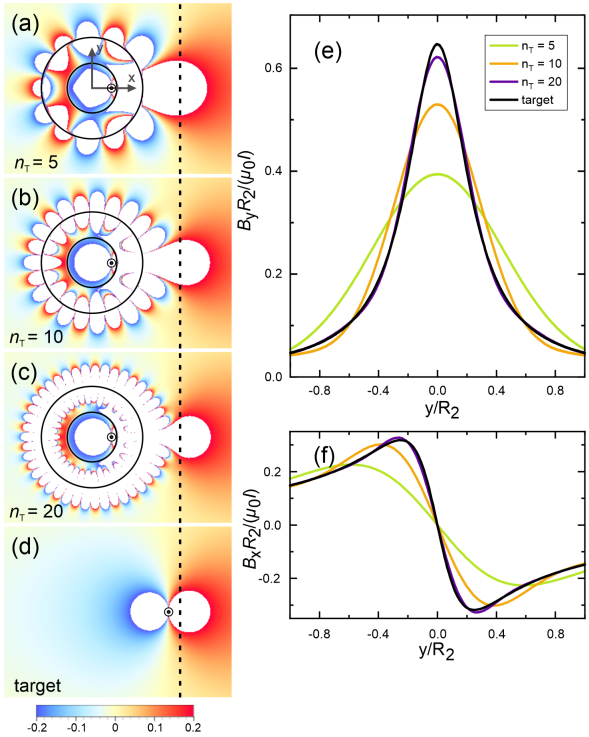

FIG. 2. (a)-(c) Plots of the normalized y-component of the magnetic induction $B_y R_2/(\mu_0 I)$ along the plane XY for a long (along z) straight wire carrying a current I placed at $(x, y) = (3/8R_2, 0)$ surrounded by the magnetization currents of a magnetic replicator of internal radius $R_1 = 1/2R_2$, external radius R_2 and relative magnetic permeability $\mu = -1$ centered at the origin of coordinates. The magnetization current density $\mathbf{K}_{M_2}$ is truncated to (a) $n_T = 5$ terms, (b) $n_T = 10$ terms, and (c) $n_T = 20$ terms. (d) Calculation of the field created by a wire with current I placed at the position of the replica, $(x, y) = (3/2R_2, 0)$. Line plots of the normalized y-component (e) and x-component (f) of the magnetic induction along the dashed line in (a)-(d) ($x = 7/4R_2$) for the cases $n_T = 5$, $n_T = 10$, $n_T = 20$, and for the replica wire.

The inspection of the role of the two current densities $\mathbf{K}_{M_1}(\varphi)$ and $\mathbf{K}_{M_2}(\varphi)$ leads to a simplification of our device. The creation of a straight replica wire carrying a current I at a distance d' from the shell center only requires a centered wire of current I and the surface current density

$$\mathbf{K}^{n_T}(\varphi) = \sum_{n=1}^{n_T} \frac{I}{\pi R_2} \left(\frac{d'}{R_2}\right)^n \cos(n\varphi)\mathbf{z} \qquad (1)$$

fed at the cylindrical surface $\rho = R_2$ (see details in Supplemental Material). Therefore, the information on the explicit values of d and R_1 are irrelevant to our experimental implementation. The examination of Eq. (1) shows why the quantity n_T cannot be made arbitrarily large when trying to create a wire at a distance from the replicator. If $d' > R_2$ the summation in Eq. (1) is dominated by its last term, which has two relevant

implications. First, larger values of n_{T} require higher current densities $\mathbf{K}^{n_{\mathrm{T}}}(\varphi)$, which for large d'/R_2 factors or large n_{T} values may be unattainable in practice. Second, the current density varies with the angular position as $\cos(n_{\mathrm{T}}\varphi)$. This means that the larger n_{T} is, the larger the required number of currents one needs to place at $\rho = R_2$, which for large n_{T} values would require a precise experimental method for positioning the wires at the surface of the replicator.'

For the experimental emulation of a current-carrying wire at a distance, we constructed a cylindrical magnetic replicator of external radius $R_2 = 40$ mm and height 400 mm. We set the replica wire current to $I = -0.5$A (the negative sign indicates the current flows in the negative $z-$direction) and its position to $d' = 60$ mm. We truncated the summation in Eq. (1) up to $n_{\mathrm{T}} = 10$. The resulting continuous sheet current density was converted into a discrete set of 20 straight current wires (current values and exact position of the wires can be found in Methods). Figure 3(a) shows the field distribution obtained with numerical calculations when considering this discrete set of wires surrounding a centered wire of current $I = -0.5$ A. The magnetic field was measured in the rectangular region delimited in Fig. 3(a) using two miniature fluxgate magnetometers. The experimental results match very well with the results calculated numerically for the metamaterial device, which confirms that the magnetization currents of a shell with negative permeability can be used to create magnetic sources at a distance [Figs. 3(b) and 3(c)].

The creation of magnetic sources at a distance provides a new strategy for focusing magnetic fields in inaccessible volumes. Imagine a strong focusing of magnetic fields is required in a region where magnetic field sources cannot be placed, e.g. inside the body of a patient. One can place a magnetic replicator in the accessible volume (outside the body of that patient) in order to emulate the field of an image wire carrying a current I close to the region where the focusing is required. Let us assume that the inaccessible region is $x > x_{\mathrm{IN}}$ and that the surface of the magnetic replicator is placed just at the border of the inaccessible region (the device is centered at the origin of coordinates and its radius is $R_2 = x_{\mathrm{IN}}$). The magnetic field distribution along different $y-$lines in the inaccessible region obtained using this strategy shows a much sharper peak than the field distribution that would be obtained by simply placing a wire with current I at $x = x_{\mathrm{IN}}$ [Fig. 4(a)]. The gradient of the field, $\partial B_y/\partial y$ is thus greatly increased.

Moreover, we experimentally demonstrated that the field created by a magnetic source can be cancelled remotely by a magnetic replicator. Together with our metamaterial device, we placed a straight wire of current $I = 0.5$ A in the position of the replica wire (which we call the "target wire"). The superposition of the field generated by the wire and that generated by the metamaterial cancel out. The experimental measurements give a very low magnetic field strength in the region $\rho > d'$ [Fig. 4(b)]. This demonstrates that magnetic sources placed in inaccessible regions (like the interior of a wall, for example) can be cancelled remotely, without the need for surrounding them with magnetic cloaks. These experimental results demonstrate the ability our replicator has to focus and cancel magnetic fields at distance. It is worth stressing that our experimental setup is, in practice, also limited by different factors. As discussed in more detail in the supplementary material, the inaccurate positioning of the different wires forming the replicator and the finite tilt of the whole structure (whose radius is much smaller than its height) explain the discrepancies between the analytical calculations and the experimental measurements.

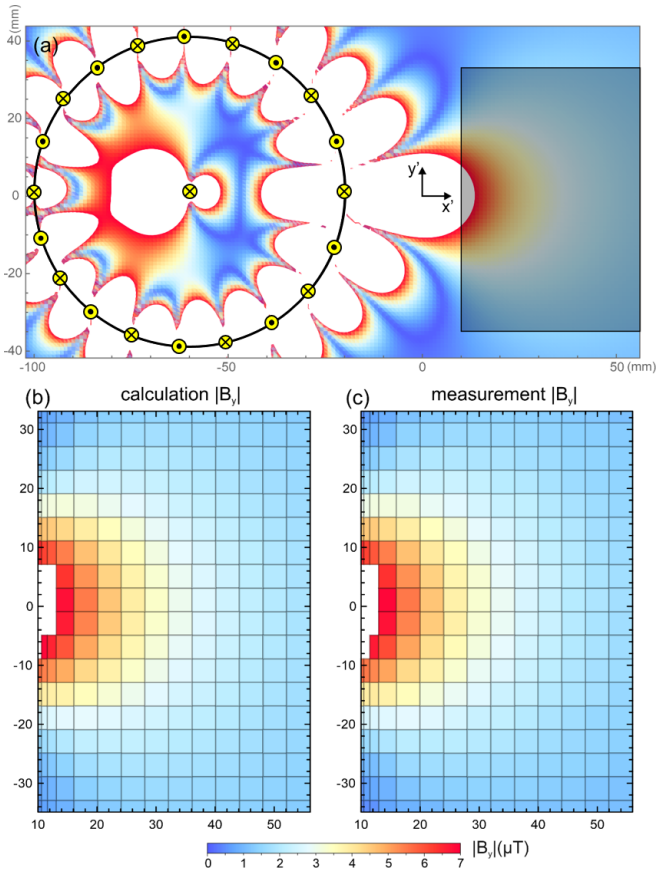

FIG. 3. (a) Calculated field $|B_y|$ created by the 21 currents (yellow dots) forming the replicator with $R_2 = 40$mm and $d' = 60$mm. The calculation assumes the wires have a length (in z) of 400mm. The shaded rectangle indicates the measured area. (b) $|B_y|$ field calculated at the positions of the measurements. (c) Measured field $|B_y|$. Standard errors associated with the measurements can be found in the Supplemental Material; values are smaller than 0.025μT everywhere.

The magnetic replicator we propose, similar to parity-time perfect lenses for electromagnetic waves [17, 18], does not require the design of bulk metamaterials with

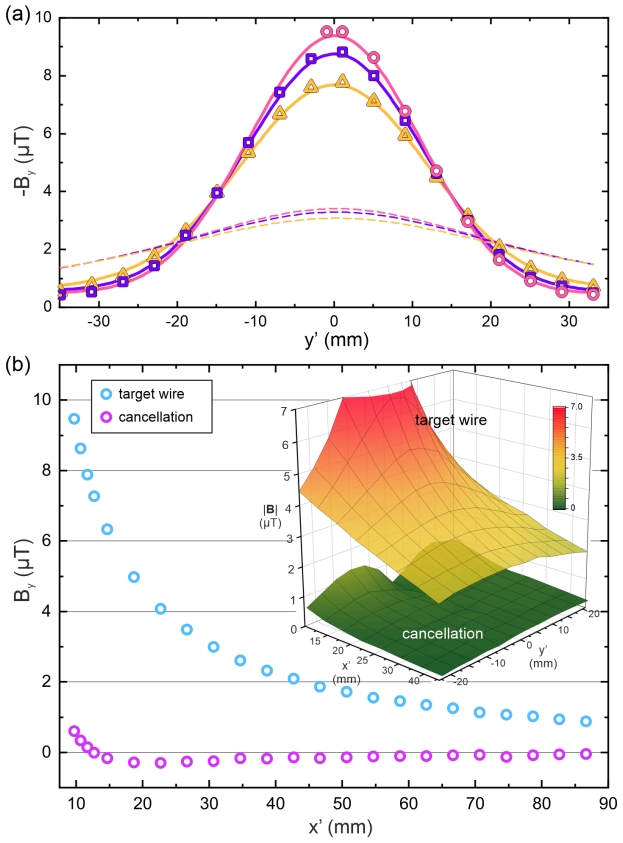

FIG. 4. (a) Plots of $-B_y$ along different parallel lines at $x' = 9.1, 10.1$ and 12.1mm (pink-circles, purple-squares, and yellow-triangles, respectively). Measurements are shown in symbols and the corresponding calculations in solid lines. Dashed lines are calculations of the field created by a single finite wire carrying a current $I = -0.5$A located at $x' = -20$mm, $y' = 0$. (b) Measurements (line $y' = 0$mm) of the field created by a wire located at the position of the image wire ("target wire") and of the field created by the magnetic replicator and the target wire ("cancellation"). Error bars (standard errors) are smaller than the symbol size. Insets show the measured $|\mathbf{B}|$ for the target wire and the cancellation configurations. The black grid shows the measurement points; the color surface is obtained as a linear interpolation between them. Standard errors are smaller than 0.02μT.

cumbersome magnetic permeability distributions; it can be realized by a precise arrangement of current-carrying electric wires. Thus, some of the issues associated with magnetic metamaterials, such as the non-linearity of their constituents [19], are avoided.

Even though our results have been demonstrated for static magnetic fields, this same device could work for low-frequency AC fields [20]. For time-dependent magnetic fields with associated wavelengths larger or comparable to the size of the device (for which the induced electric fields can be neglected), one could feed AC currents to the same active metamaterial. Thus, our experimental setup would maintain its functionality up to frequencies around 100MHz.

The emulation of a magnetic source at distance is valid everywhere in space except in the circular region delimited by the position of the replica source and can be made as exact as desired at the expense of increased complexity and power requirements. As mentioned above, not only the amount of wires but also the current each of them carries increases with the chosen n_{T}; the current carried by the wire at $(x, y) = (R_2, 0)$, for example, increases with n_{T} as $(d'/R_2)^{n_{\mathrm{T}}}$. Therefore, the currents and the required power to create a source at a distance rapidly increase with the distance of the target source (d'/R_2) as well as with the total number of terms in $\mathbf{K}^{n_{\mathrm{T}}}$. In scenarios where high field accuracy and strength are demanded, high-T_c superconductors could be used to create the circuits forming the metamaterial.

In spite of considering translational symmetry along the $z-$direction throughout the article, these same ideas could be applied to emulate a 3D magnetic source, like a point magnetic dipole. In that case, one could consider a spherical shell with negative permeability and calculate the corresponding magnetization currents, which would likely result in cumbersome inhomogeneous distributions of surface and volume current densities.

Results presented here open a new pathway for controlling magnetic fields at a distance, with potential technological applications. For example, a wide variety of microrobots and functional micro/nano-particles are moved and actuated by means of magnetic fields [6, 21–24]. They can perform drug transport and controlled drug release [7], intraocular retinal procedures [22], or even stem cell transplantation [25]. However, the rapid drop off of field strength with target depth within the body is acknowledged to pose severe limitations to the clinical development of some of them [6, 7]. Another example is transcranial magnetic stimulation (TMS), which uses magnetic fields to modulate the neural activity of patients with different pathology [8]. In spite of its success, TMS suffers from limited focality, lacking the ability to stimulate specific regions [8]. Our results could benefit both technologies by enabling the precise spatial targeting of magnetic fields at the required depth inside the body. In actual applications, though, one should take into account that the region between the metamaterial and the replica image would experience strong magnetic fields. Another area of application is in atom trapping. Depending on the atom's state, they can be trapped in magnetic field minima (low-field seekers) or maxima (high-field seekers). Since local maxima are forbidden by Earnshaw's theorem, high-field seekers are typically trapped in the saddle point of a magnetic potential that oscillates in time [26]. However, these dynamic magnetic traps are shallow compared to traps for low-field seekers [27, 28]. By emulating a magnetic source at distance, one would be able to generate magnetic potential landscapes with higher gradients at the desired target position resulting in tighter traps.

In conclusion, our results demonstrate that a shell with negative permeability can emulate and cancel magnetic sources at distance. This ability to manipulate magnetic fields remotely will enable both the advancement of existing technology and potentially new applications that require the tailoring of magnetic fields in inaccessible regions.

J.P.C is funded by a Leverhulme Trust Early Career fellowship (ECF-2018-447). We thank P. Maurer, I. Hughes and C. Navau for their feedback on the article.

* rosa.machbatlle@iit.it

[1] S. Narayana and Y. Sato, DC Magnetic Cloak, Advanced Materials **24**, 71 (2012).

[2] F. Gömöry, M. Solovyov, J. Souc, C. Navau, J. Prat-Camps, and A. Sanchez, Experimental realization of a magnetic cloak., Science (New York, N.Y.) **335**, 1466 (2012).

[3] C. Navau, J. Prat-Camps, O. Romero-Isart, J. Cirac, and A. Sanchez, Long-Distance Transfer and Routing of Static Magnetic Fields, Physical Review Letters **112**, 253901 (2014).

[4] J. Prat-Camps, C. Navau, and A. Sanchez, A Magnetic Wormhole, Scientific Reports **5**, 12488 (2015).

[5] J. Jeans, General analytical theorems, in *Mathematical Theory of Electricity and Magnetism*, Cambridge Library Collection - Physical Sciences (Cambridge University Press, 2009) p. 156–184, 5th ed.

[6] M. Sitti, Miniature devices: Voyage of the microrobots, Nature **458**, 1121 (2009).

[7] J. Estelrich, E. Escribano, J. Queralt, and M. Busquets, Iron oxide nanoparticles for magnetically-guided and magnetically-responsive drug delivery, International journal of molecular sciences **16**, 8070 (2015).

[8] T. Wagner, A. Valero-Cabre, and A. Pascual-Leone, Noninvasive human brain stimulation, Annual Review of Biomedical Engineering **9**, 527 (2007).

[9] R. Mach-Batlle, A. Parra, S. Laut, N. Del-Valle, C. Navau, and A. Sanchez, Magnetic Illusion: Transforming a Magnetic Object into Another Object by Negative Permeability, Physical Review Applied **9**, 034007 (2018).

[10] V. G. Veselago, The electrodynamics of substances with simultaneously negative values of ε and μ, Soviet Physics Uspekhi **10**, 509 (1968).

[11] O. Dolgov, D. Kirzhnits, and V. Losyakov, On the admissible values of the static magnetic permeability, Solid State Communications **46**, 147 (1983).

[12] R. Mach-Batlle, A. Parra, J. Prat-Camps, S. Laut, C. Navau, and A. Sanchez, Negative permeability in magnetostatics and its experimental demonstration, Physical Review B **96**, 094422 (2017).

[13] J. B. Pendry and S. A. Ramakrishna, Near-field lenses in two dimensions, Journal of Physics: Condensed Matter **14**, 8463 (2002).

[14] J. Pendry, Perfect cylindrical lenses, Optics Express **11**, 755 (2003).

[15] S. Anantha Ramakrishna and J. B. Pendry, Spherical perfect lens: Solutions of Maxwell's equations for spherical geometry, Physical Review B **69**, 115115 (2004).

[16] G. W. Milton, N. A. P. Nicorovici, R. C. Mcphedran, and V. A. Podolskiy, A proof of superlensing in the quasistatic regime, and limitations of superlenses in this regime due to anomalous localized resonance, Proceedings of the Royal Society A: Mathematical, Physical and Engineering Sciences **461**, 3999 (2005).

[17] R. Fleury, D. L. Sounas, and A. Alù, Negative refraction and planar focusing based on parity-time symmetric metasurfaces, Physical Review Letters **113**, 10.1103/PhysRevLett.113.023903 (2014).

[18] F. Monticone, C. A. Valagiannopoulos, and A. Alù, Parity-time Symmetric nonlocal metasurfaces: All-angle negative refraction and volumetric imaging, Physical Review X **6**, 10.1103/PhysRevX.6.041018 (2016).

[19] J. M. Coey, *Magnetism and magnetic materials* (Cambridge university press, 2010).

[20] J. Prat-Camps, C. Navau, and A. Sanchez, Quasistatic Metamaterials: Magnetic Coupling Enhancement by Effective Space Cancellation, Advanced Materials **28**, 4898 (2016).

[21] R. Dreyfus, J. Baudry, M. L. Roper, M. Fermigier, H. A. Stone, and J. Bibette, Microscopic artificial swimmers, Nature **437**, 862 (2005).

[22] M. P. Kummer, J. J. Abbott, B. E. Kratochvil, R. Borer, A. Sengul, and B. J. Nelson, Octomag: An electromagnetic system for 5-dof wireless micromanipulation, IEEE Transactions on Robotics **26**, 1006 (2010).

[23] W. Hu, G. Z. Lum, M. Mastrangeli, and M. Sitti, Small-scale soft-bodied robot with multimodal locomotion, Nature **554**, 81 (2018).

[24] Y. Kim, H. Yuk, R. Zhao, S. A. Chester, and X. Zhao, Printing ferromagnetic domains for untethered fast-transforming soft materials, Nature **558**, 274 (2018).

[25] S. Jeon, S. Kim, S. Ha, S. Lee, E. Kim, S. Y. Kim, S. H. Park, J. H. Jeon, S. W. Kim, C. Moon, *et al.*, Magnetically actuated microrobots as a platform for stem cell transplantation, Science Robotics **4**, eaav4317 (2019).

[26] E. A. Cornell, C. Monroe, and C. E. Wieman, Multiply loaded, ac magnetic trap for neutral atoms, Physical review letters **67**, 2439 (1991).

[27] J. Fortágh and C. Zimmermann, Magnetic microtraps for ultracold atoms, Reviews of Modern Physics **79**, 235 (2007).

[28] E. A. Hinds and I. G. Hughes, Magnetic atom optics: mirrors, guides, traps, and chips for atoms, Journal of Physics D: Applied Physics **32**, R119 (1999).